

Huygens Probe descent dynamics inferred from Channel B signal level measurements

Y. Dzierma^{a,*}, M.K. Bird^a, R. Dutta-Roy^a, Miguel Pérez-Ayúcar^b,
D. Plettemeier^c, P. Edenhofer^d

^aArgelander-Institut für Astronomie, Universität Bonn, Auf dem Hügel 71, 53125 Bonn, Germany

^bESA-ESTEC, Keplerlaan 1, 2200 AG Noordwijk, Netherlands

^cElektrotechnisches Institut, Technische Universität Dresden, 01062 Dresden, Germany

^dInstitut für HF-Technik, Universität Bochum, 44780 Bochum, Germany

Accepted 13 April 2007

Available online 27 April 2007

Abstract

The signal strength of the Huygens Probe Channel B transmission to the Cassini Orbiter was monitored during the Probe descent through Titan's atmosphere on 14 January 2005. A model of the Probe motion during the mission was constructed to include Probe spin, coning motion and tilt caused by varying wind speeds. This simple model is sufficient to reproduce the most prominent features seen in the signal level measurements. It provides estimates of the coning and tilt angles as well as the direction of the Huygens coordinate axes over extended time intervals in the mission.

© 2007 Elsevier Ltd. All rights reserved.

Keywords: Titan; Huygens; Radio science; Probe dynamics

1. Introduction

The Huygens Probe separated from the Cassini Orbiter on Christmas Day 2004 and followed a ballistic trajectory that impacted Titan on 14 January 2005 (Lebreton et al., 2005). The proper attitude at entry into Titan's atmosphere was achieved by imparting a spin to Huygens at the moment of separation from Cassini. The spin rate at this instant was 7.5 rpm and the sense of rotation was counter-clockwise as seen from Cassini along the direction of the Probe's velocity. After entry into the high atmosphere, Huygens was decelerated by means of a heat shield to Mach 1.5 (400 m/s in the Titan atmosphere), at which point the pilot parachute was deployed, thereby pulling off the aft cover and releasing the main parachute. This event, denoted ' t_0 ', marked the beginning of the Huygens descent

sequence. The Probe was then sufficiently slowed to allow separation from the decelerator heat shield, and transmission of data to the Orbiter was initiated at $t_0 + 46$ s. The main parachute was replaced by a smaller drogue chute at 15 min mission time in order to shorten the duration of the descent to a time of 2 h 15 min \pm 15 min. The actual descent time was 2 h 27 min 50 s (8870 s) with the landing occurring at 11:38:11 UTC/SCET.

Huygens continually transmitted data to the Cassini Orbiter via its Channels A and B, operating at frequencies of 2040 and 2098 MHz, respectively. Due to an omitted command in the mission command line to the Probe receivers on Cassini, the Channel A receiver was not properly configured and was unable to lock onto the signal. All data on Channel A, including the signal power and the received frequency, the primary data of the Huygens Doppler Wind Experiment (DWE), were lost. It was fortunate that measurements of the Channel A carrier signal, driven by a DWE-supplied Ultra-Stable Oscillator on board Huygens, could be recorded by large radio telescopes on Earth to recover the main DWE science goal, a height

*Corresponding author.

E-mail address: ydzierma@geophysik.uni-kiel.de (Y. Dzierma).

¹Now at: Geophysikalisches Institut, Universität Kiel, Otto-Hahn-Platz 1, 24106 Kiel, Germany.

profile of Titan’s zonal winds (Bird et al., 2005). The Channel A amplitude data were of limited use for studying Probe dynamics because of the low signal level and long sample time ($\Delta t \approx 2$ s). In contrast, Channel B Doppler and amplitude data were recorded at a rate of eight samples per second over the entire descent time. The Channel B frequency data, dominated by the uncalibrated drift characteristics of the transmitter’s standard oscillator, cannot be used for a determination of the Probe velocity. This work reports the results of studies of the Channel B signal strength at Cassini, as measured by the automatic gain control (AGC), which provides insight into the attitude of the Probe with respect to the Orbiter during the descent.

2. Channel B signal level measurements

The Huygens Channel B AGC measurements over the duration of the descent are shown in Fig. 1 (upper panel).

Short time-scale periodic variations in the observed Channel B AGC (e.g., lower panels in Fig. 1) are mainly caused by the rotation of the Probe and can be used to determine the instantaneous Probe spin rate and spin phase during the descent. The Probe spin rate can be found either from the periodicity of the AGC variations at specific times or from a dynamic power spectrum of the AGC measurements as shown in Fig. 2 (Dzierma, 2005; Sarlette, 2005). In combination with the spin measurements from the Huygens Radial Accelerometer Sensor Unit (RASU), these were used by the Huygens Project Science Team (PST) to determine the mission spin profile, shown in Fig. 3 (Lebreton et al., 2005). The profile shows marked variations in spin rate and a reversal in spin direction after about 10 min in the mission. The surprising reversal, which was not envisioned in pre-flight scenarios and has not been satisfactorily explained so far, was clearly confirmed by detailed analysis of the AGC variations over a rotational

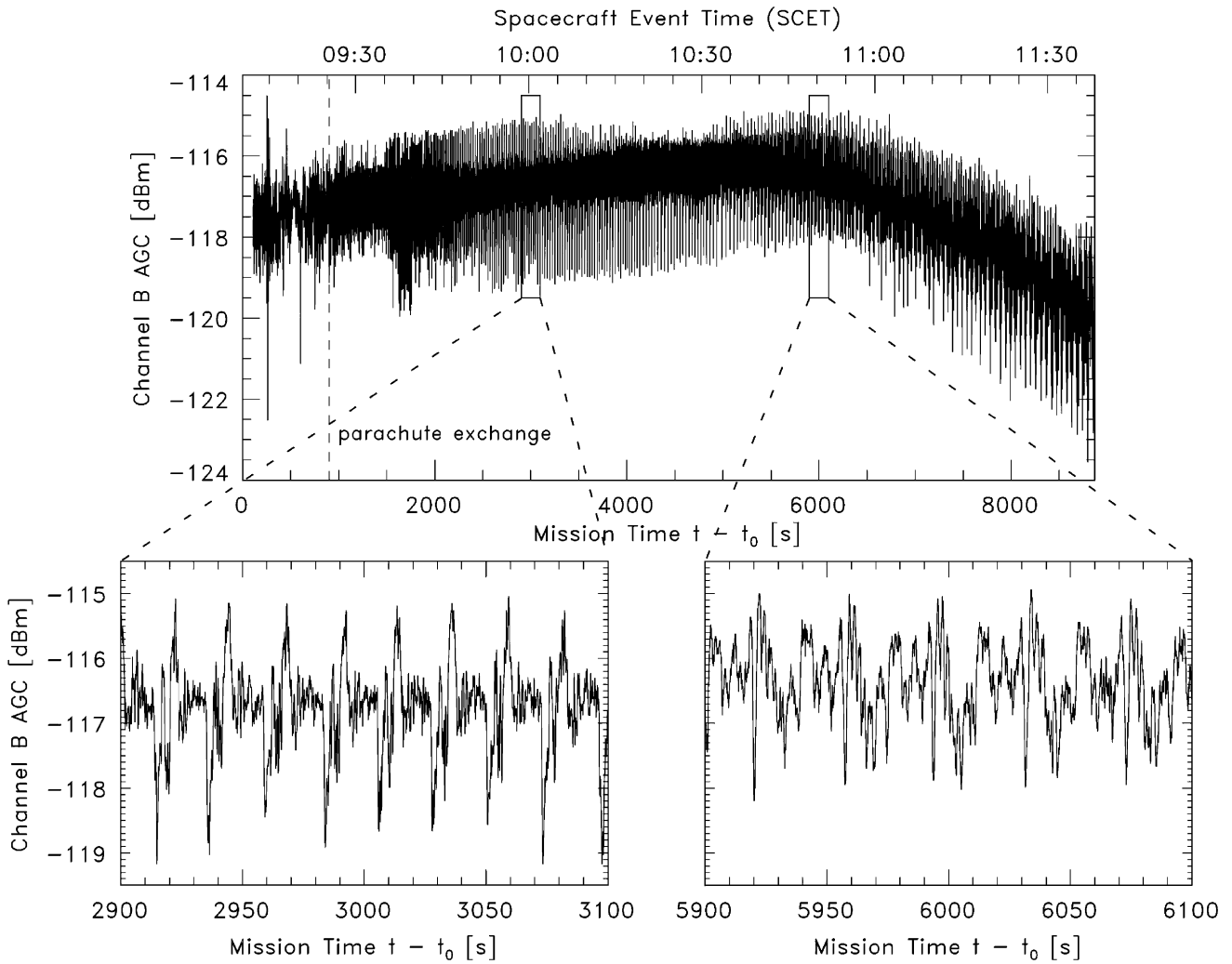


Fig. 1. Upper panel: Channel B AGC measured on Cassini from the start of the Probe transmission to the nominal impact at 8870 s mission time. The sampling rate is 8 samples per second. Short time-scale AGC variations are not visible in this representation. The lower panels show the AGC profile at higher resolution for two specific times in the mission when the spin period could be determined by simple inspection. Lower left: Channel B AGC during a 200 s interval near mission time 3000 s. Lower right: Channel B AGC during a 200 s interval near mission time 6000 s.

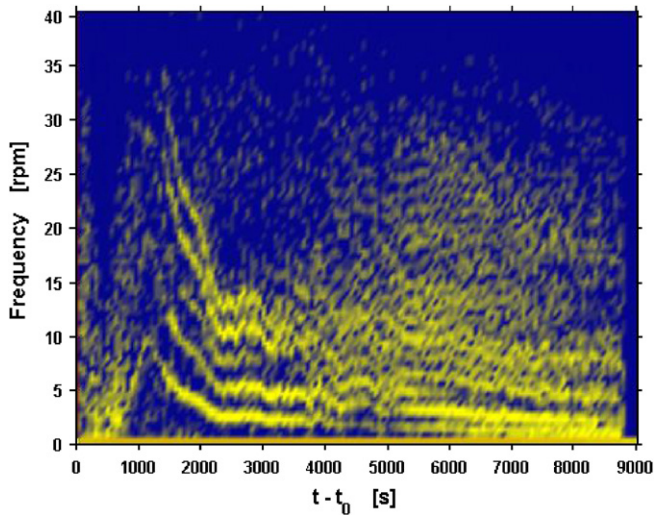


Fig. 2. Dynamic power spectrum of the Channel B AGC measured on Cassini. The power spectral density is plotted as a function of frequency (in rotations per minute) and mission time, with a time resolution of 1 min. Brighter colours indicate higher power spectral density. The fundamental mode (maximum: ≈ 10 rpm near mission time 1250 s) and several higher harmonics are clearly visible during much of the descent. The dominant frequencies clearly change over the course of the descent with the probe spin rate. Several similar plots were used to bring out weak features in selected intervals; the results were then combined to determine the spin rate at nearly all times.

period and simulated by models shown and discussed below (for more details, see Sarlette, 2005; Dzierma, 2005).

3. Channel B AGC model

The long time-scale AGC variations (as seen in the minimum and maximum AGC envelopes in Fig. 1) reflect the changing geometry of the Probe–Orbiter line-of-sight. In order to simulate the observed Channel B AGC profile during descent, including both long and short time-scale variations, a model was constructed that is based on:

- the known position and distance of the Cassini Orbiter with respect to the Huygens Probe, provided by the Cassini Navigation Team (NASA) and the Huygens Descent Trajectory Working Group (DTWG—Kazemi-nejad et al., 2007),
- the spin rate of the Probe as provided by the Huygens PST (Fig. 3),
- the Cassini high gain antenna (HGA) peak gain of 34.7 dBi (Jones and Giovagnoli, 1997),
- the Huygens Probe antenna nominal transmitted power of 40.7 dBm (Jones and Giovagnoli, 1997) and calibrated antenna pattern (measured during pre-launch tests, Fig. 4).

This model allows one to account for the effects of:

- coning motion of the Probe caused by misalignment, i.e., a constant precession of the Probe's

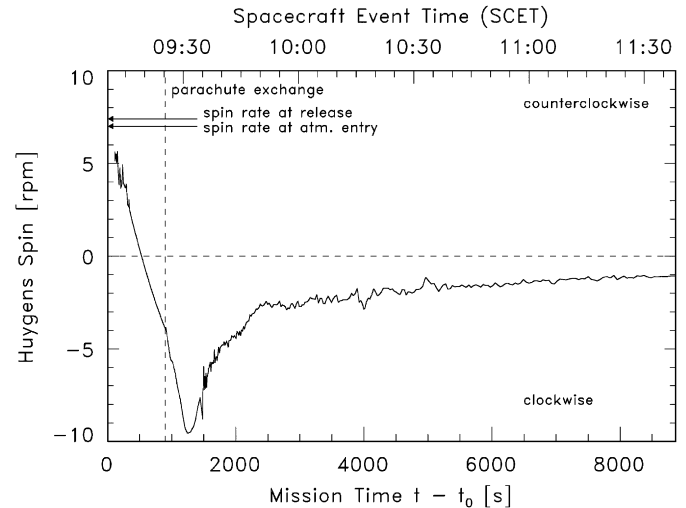


Fig. 3. Spin rate profile of the Huygens Probe during descent, as provided by the Huygens PST (Lebreton et al., 2005). This spin profile was used for all simulations of the Probe AGC. The Probe entered the Titan atmosphere with nearly the same spin rate and spin direction imparted at its separation from the Cassini Orbiter, i.e., about 7.5 rpm in the counterclockwise direction. The spin reversal early in the mission was not predicted in the pre-flight scenarios. A simple comparison of the periodic variations in the Probe AGC with the variations in the Probe antenna pattern over one period (at the known Probe aspect angle) shows that while the spin early in the mission was counterclockwise, it clearly reversed later in the descent (Dzierma, 2005). The same conclusion is reached using the refined AGC model presented in this work. Note also the sudden increase in the spin rate associated with the higher descent velocity following parachute exchange.

nominally vertical body axis (x -axis) about the true spin axis,

- tilt of the Probe, i.e., a deviation of the nominally vertical spin axis from the local vertical due to external force effects (e.g., winds).

The initial azimuth (spin phase) of the Probe at the start of the mission time ($t = t_0$) is unknown and remains a free parameter that is chosen to obtain the best fit of the model to the observations. The Probe axes are defined such that the Probe x -axis (nominal spin axis) points vertically upward from the experiment platform; the z -axis is aligned with the DISR imager (Fig. 5).

4. AGC simulations and observational comparison

The measured Channel B AGC over the whole mission is compared with the model predictions for coning angles 0° , 5° and 10° in Fig. 6. Whereas the temporal variation of the AGC is particularly sensitive to the magnitude of the coning angle, the effects of the coning direction (coning azimuth) and the initial Probe spin phase are minor. This is due to the fact that the large variations in amplitude are primarily caused by the change in the Probe aspect angle (PAA), which is essentially the elevation of the Huygens-to-Cassini line-of-sight vector in the Probe antenna diagram. This dominates variations caused by the

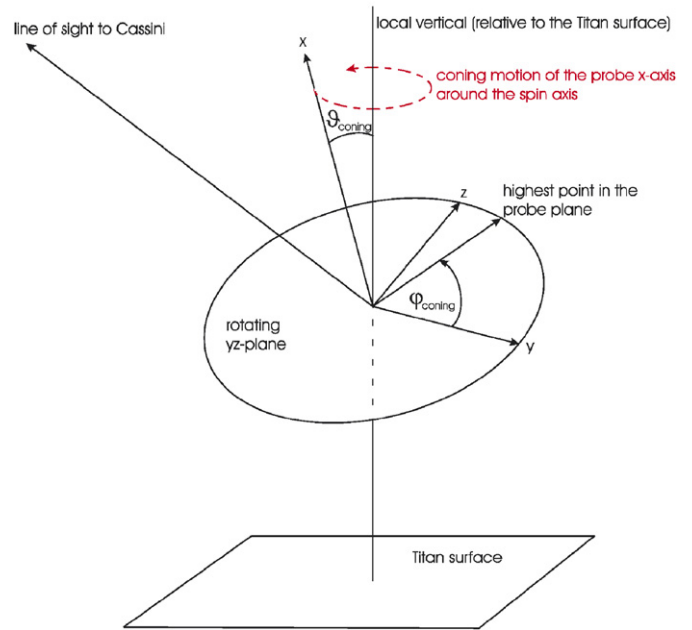
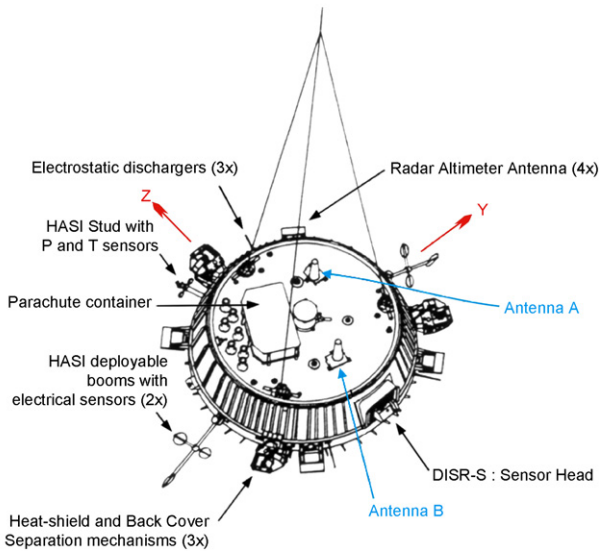
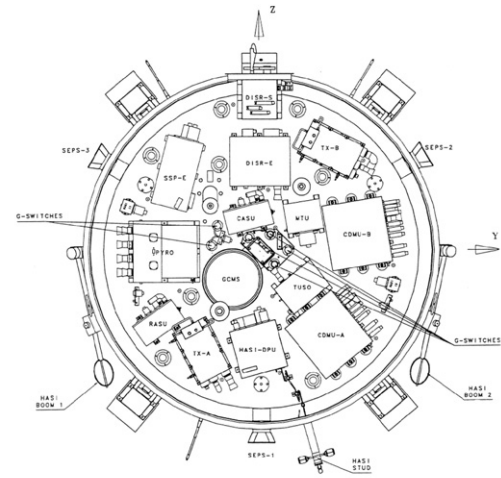
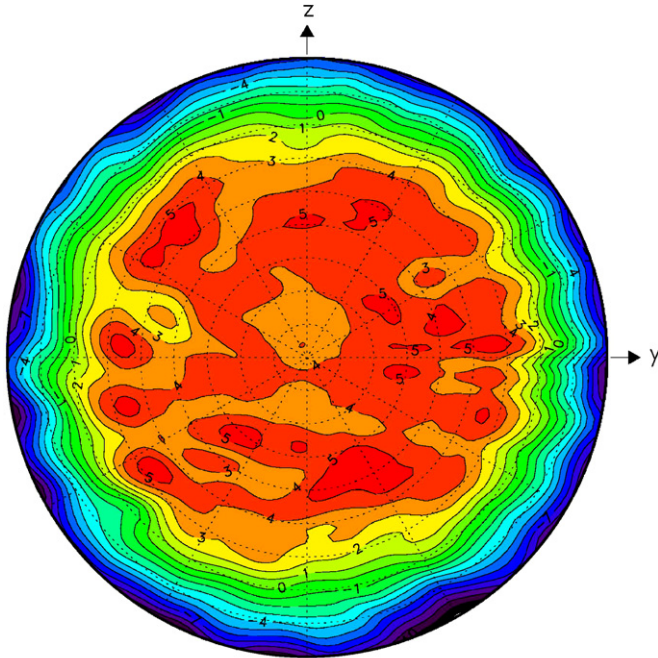


Fig. 4. Upper panel: Huygens Probe Transmitter Channel B antenna pattern from pre-flight measurements on a full-scale mock-up. The Probe antenna gain depends on the direction of the line-of-sight vector from Probe to Orbiter. This vector can be parameterized by two angles: (a) the Probe aspect angle θ (PAA), measured from local vertical at the Probe, and (b) the spin phase, or azimuth ϕ , which is defined in the horizontal Probe platform, measured in the mathematically positive sense from the y -axis. The 3dB-beamwidth (FWHM) of the Probe antenna is nominally 120° , but extends out to 140° at favourable values of ϕ . Concentric circles in the figure denote constant PAA values at 10° intervals. The outer edge is at PAA 90° . The gain contours are given in decibels relative to isotropic (dBi). Lower panel: Huygens as seen from above, indicating the position of the telemetry antennas for Channels A and B (Lebreton and Matson, 1997). The position of the axes has been indicated for easier comparison with Fig. 5.

Fig. 5. Upper panel: top view of the Huygens experiment platform in the descent module, showing the alignment of the Huygens coordinate axes (Lebreton and Matson, 1997). The x -axis points vertically upward from the experiment platform; the yz -plane is the same as shown in Fig. 4 and the z -axis is aligned with the DISR camera. Lower panel: graphic representation of the coning motion of the probe and the relevant coordinates, for the simplified case where the spin axis is in its normal (vertical) orientation. The x , y and z body axes are fixed to the Probe. For coning motion the x -axis is misaligned by the coning angle θ_{coning} with the spin axis and precesses about the nominally vertical spin axis at the rotation period. There is a radial line in the yz -plane associated with the direction of x -axis tilt that defines the coning azimuth ϕ_{coning} . The line-of-sight vector to the Orbiter is projected onto the Probe plane to find the Probe aspect angle (PAA) and azimuth to Cassini. Generally, the spin axis does not need to be vertical.

rotational change in azimuth at constant PAA, since the antenna pattern is roughly symmetric about the nominal antenna boresight (x -axis).

The spin reversal at mission time 540 s is reproduced by all simulations. Apart from this feature, the model poorly simulates the measured AGC during the early part of the descent. Following the parachute exchange at mission time 900 s, the Probe enters a phase of “rough ride” (Lebreton et al., 2005), where the measured AGC is characterized by many fluctuations and irregularities that cannot be

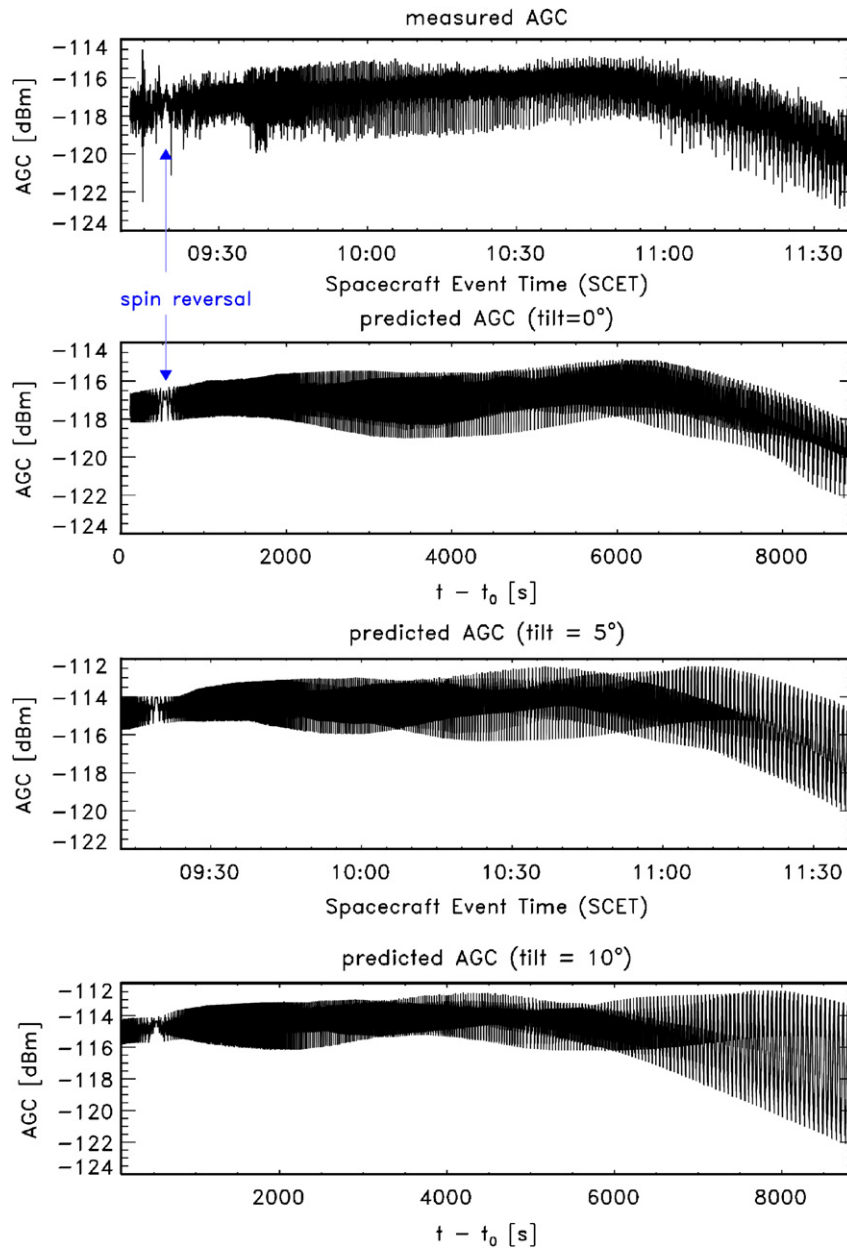


Fig. 6. Huygens Channel B AGC: observations and simulations. Upper panel: AGC measurements; lower panels: model predictions for coning angle 0° , 5° and 10° . The model calculations were performed for an initial Probe spin phase of 0° . The coning azimuth was chosen such that the Huygens y -axis points to the highest point of the experiment platform relative to the local horizontal. The coning azimuth and initial spin phase, however, are not significant for the analysis of the mission as a whole, since the overall gain variations depend mainly on the change in Probe aspect angle during the descent.

predicted by a model of smooth rotation and constant coning. Later in the descent, the AGC can be modelled to a good approximation with a coning angle near zero. Model results with large coning angles produce very large AGC variations and do not agree with observations. This disagreement is particularly pronounced near the end of the descent, i.e., for large PAA. Since the antenna gain decreases rapidly with PAA in this phase, a significant coning motion causes large gain variations over each rotation. This analysis implies that the average coning angle over the whole descent must have remained small (less than 5°). It cannot be ruled out, however, that the

coning angle could have changed slightly during the descent (e.g., if one or more parachute risers are kinked by wind gusts or temporarily tangled).

While the later part of the descent can be modelled well by non-tilted, non-coning Probe motion (pure horizontal rotation obeying the derived spin profile), the AGC in the early descent phase cannot be reproduced satisfactorily by this simple approach. This phase is expected to include some Probe buffeting and oscillating. Resonant frequencies of the Probe–parachute system seem to exist for swinging motion at 1.7–1.8 and 18 Hz, as observed in the DISR data set (see Karkoschka et al., 2007). These and other effects

cannot be modelled unless a large number of free parameters for spontaneous excitation of pendulum motion and rapid decay are included. However, it is possible to reproduce the larger-scale features in the AGC model by introducing the effect of an east–west Probe system tilt.

The Probe is accelerated and decelerated as it descends through regions of variable wind. The dominant winds on Titan over the largest part of the descent were found to be prograde (i.e., eastward) zonal winds (Bird et al., 2005; Folkner et al., 2006). When the wind speed increases with time, the Probe system (essentially the parachute in this case) undergoes a lateral acceleration to the east. This effectively tilts the Probe system to the east, away from the direction to Cassini. Analogously, winds decreasing with time produce a tilt to the west. The ratio of lateral to vertical force may be used to determine the tilt angle ϑ_{tilt} from the simple relationship

$$\tan \vartheta_{\text{tilt}} = \frac{\partial u / \partial t}{g}, \quad (1)$$

where $g = 1.35 \text{ m/s}^2$ is the gravitational acceleration on Titan’s surface (the change of g with altitude is negligible for this purpose). The zonal wind profile of Bird et al. (2005), shown in Fig. 7 (upper panel), is used to calculate the wind shear $\partial u / \partial t$. The resulting tilt angle profile is shown in Fig. 7 (lower panel). The corresponding AGC simulation is shown in Fig. 8 (upper panel). The tilt angle

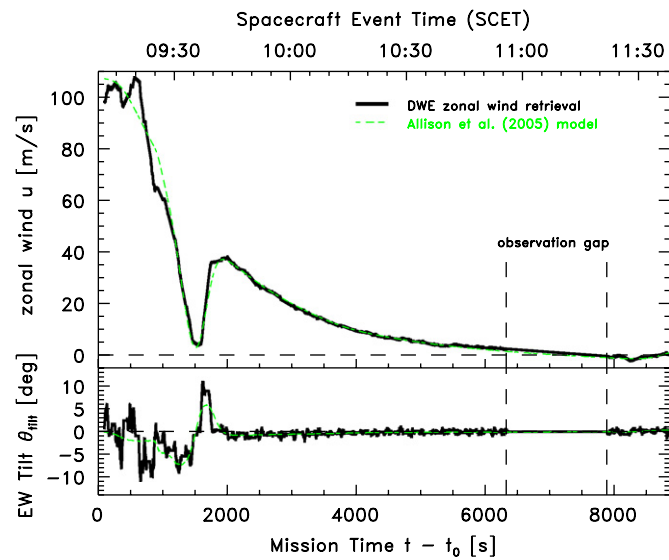


Fig. 7. Upper panel: DWE zonal wind speed during Titan descent. The solid curve shows the measurements (Bird et al., 2005); the dash-dotted curve is an analytical approximation to the DWE zonal wind (Allison et al., 2005). Positive values denote prograde zonal winds, negative values retrograde winds. The DWE zonal wind was interpolated between the end of the Green Bank Telescope observations (at about 6327 s mission time) and the onset of the Parkes Telescope observations (around 7887 s mission time). Lower panel: east–west tilt of the Probe caused by acceleration due to changing wind velocities using Eq. (1). The tilt derived from the DWE zonal wind (solid curve) was smoothed (running average) over 30 s intervals. The tilt shown by the dashed curve was derived from the Allison et al. (2005) wind profile in the upper panel.

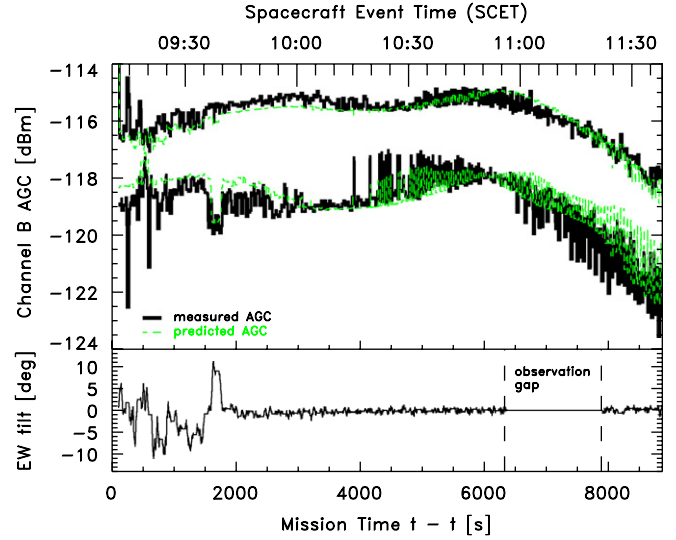


Fig. 8. Upper panel: comparison of the measured Channel B AGC (solid curve) with the model predictions for zero coning and smoothed east–west tilt based on the DWE zonal wind profile (dashed line). For better comparison, only the upper and lower envelopes of the AGC curves, averaged over 30-s intervals, are plotted. Lower panel: EW tilt estimated from the DWE zonal wind profile, smoothed over 30 s intervals (Fig. 7, lower panel). The inclusion of an east–west tilt of the Probe significantly improves the model fit to the observations, particularly in the region of strong wind shear around 1500 s mission time. It is also evident that the fit of the predicted AGC to the observations is poor in the gap between Green Bank and Parkes Telescope observations, where no direct observations of wind speed—and hence of tilt—are available. This suggests that the wind-induced tilt is significant for the quality of the fit, perhaps even in regions where no large wind shear is supposed to exist. A few excursions in the predicted AGC near the end of the mission are most probably due to our incomplete knowledge of the antenna side lobes at large PAA.

during descent is shown again for comparison in the lower panel of Fig. 8.

Instead of using the DWE zonal speed profile (Bird et al., 2005), an analytical approximation by Allison et al. (2005), also shown in Fig. 7 (upper panel), can be used with the same approach for determining the tilt from the derivative of the zonal wind speed (Fig. 7, lower panel). The results of this smoothed model fit the observations well over large parts of the descent. In the region of large wind shear, however, the more abrupt change in wind speed and tilt from the DWE observations model can better explain the observed sharp AGC variations.

The meridional winds on Titan have been found to be small, at least at altitudes below about 45 km, and the north–south tilt under the main parachute was estimated to be about 60% of the east–west tilt (Karkoschka et al., 2007). Simulations including the additional north–south tilt do not differ considerably from simulations neglecting north–south tilt, demonstrating that the AGC at these times is insensitive to the north–south tilt. While the overall motion of the Probe during descent seems well described by the simple rotation model including wind-induced tilt, pendulum motion excited by turbulence, which decays rapidly, cannot be ruled out.

The analysis of the mission as a whole has concentrated so far only on the PAA, which reflects the influence of tilt/coning motion of the Probe. When considering only a few periods at a time, the azimuth of the line-of-sight vector in the antenna diagram plays an important role in the fit. In Fig. 9, we compare the model predictions with the AGC measurements at 3000 s mission time. The fit for 0° coning is so good that the directions of the Probe axes are known at all times during this phase of the descent. Furthermore, this simulation shows that the AGC pattern can only be explained by clockwise rotation of the Probe. The path described by the line-of-sight vector to Cassini in the antenna diagram during this period is also displayed in Fig. 9 (right panel) for the case of no coning.

A similar analysis was carried out over the whole mission, considering only a few periods at a time. The uncertainty in determining the best-fit coning angle and coning azimuth for cases of good fit is about 3° in coning angle and $5\text{--}15^\circ$ in coning azimuth and initial spin phase. While the fits sometimes agree very well with the data and the free parameters (initial spin phase, coning angle and coning azimuth) can be held nearly constant over long times, the fit can suddenly be lost at other times. It can either be replaced by a different set of parameters a short while later or the same fit reappears after a small interruption which cannot be plausibly matched by any model. This may be an indication for pendulum motion of the Probe caused by wind buffeting and turbulence. Indeed, some particular rotation periods can only be fit

satisfactorily by including a non-negligible tilt. An example with a best-fit tilt of 8° is shown in Fig. 10. This is in agreement with the coning angle derived from the central and radial accelerometer sensor unit readings (CASU and RASU), which indicate a rough division of the descent into three phases: a calm descent under the main parachute ($0\text{--}4^\circ$ coning angle), a rough descent with the stabilizer chute ($4\text{--}9^\circ$ coning) and finally a moderately calm late descent with the stabilizer chute ($1\text{--}5^\circ$) (Pérez-Ayúcar et al., 2005). A more detailed analysis of the short-term motion of the probe, the mean tilt angles and probe stability from SSP measurements is given by Lorenz et al. (2007).

5. Huygens impact on Titan's surface

The small-scale AGC variations are difficult to model unambiguously at late times in the descent because of the increasingly larger value of the PAA. There is thus a large uncertainty in the predicted Probe azimuth at impact. Small tilt and small coning angles ($<5^\circ$) now play a more important role in the resulting AGC simulation. On the other hand, no role is played by the wave reflected from Titan's surface (Pérez-Ayúcar et al., 2006) in the final few minutes before impact. It can be shown that the reflected wave power during the last rotation (altitude below 300 m) is at least 15 dB below that of the direct signal power for all values of azimuthal orientation.

Fig. 11 shows the AGC predicted for simple rotation superimposed onto the observed Channel B AGC for the

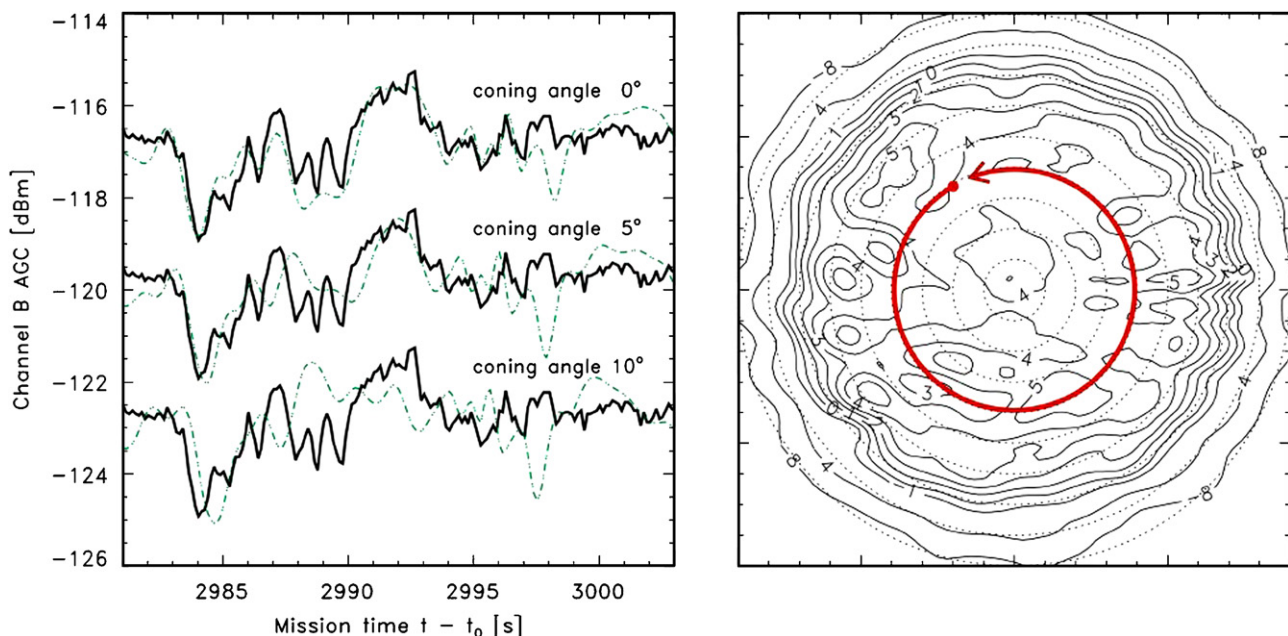


Fig. 9. Left panel: comparison of the measured Channel B AGC with the model results for different coning angles at approximately 10:00 UTC (around 3000 s mission time). The measured AGC (solid curves) is compared with simulations with coning angles of 0° , 5° and 10° , respectively (dashed curves). The latter two comparisons are lowered by 3 and 6 dB for clarity. The model with a coning angle of 0° is in best agreement with the data. Right panel: path described by the Huygens/Cassini line-of-sight vector in the antenna diagram during the time plotted, for the best-fit case of zero coning. The dot corresponds to mission time 2981 s (start time in the left panel); the arrowhead gives the position of the line-of-sight vector at mission time 3003 s (end time in the left panel) and denotes the direction of movement of the line-of-sight vector in the antenna diagram. For counterclockwise rotation, the AGC time series over each period would be approximately reversed and would not fit the measurements.

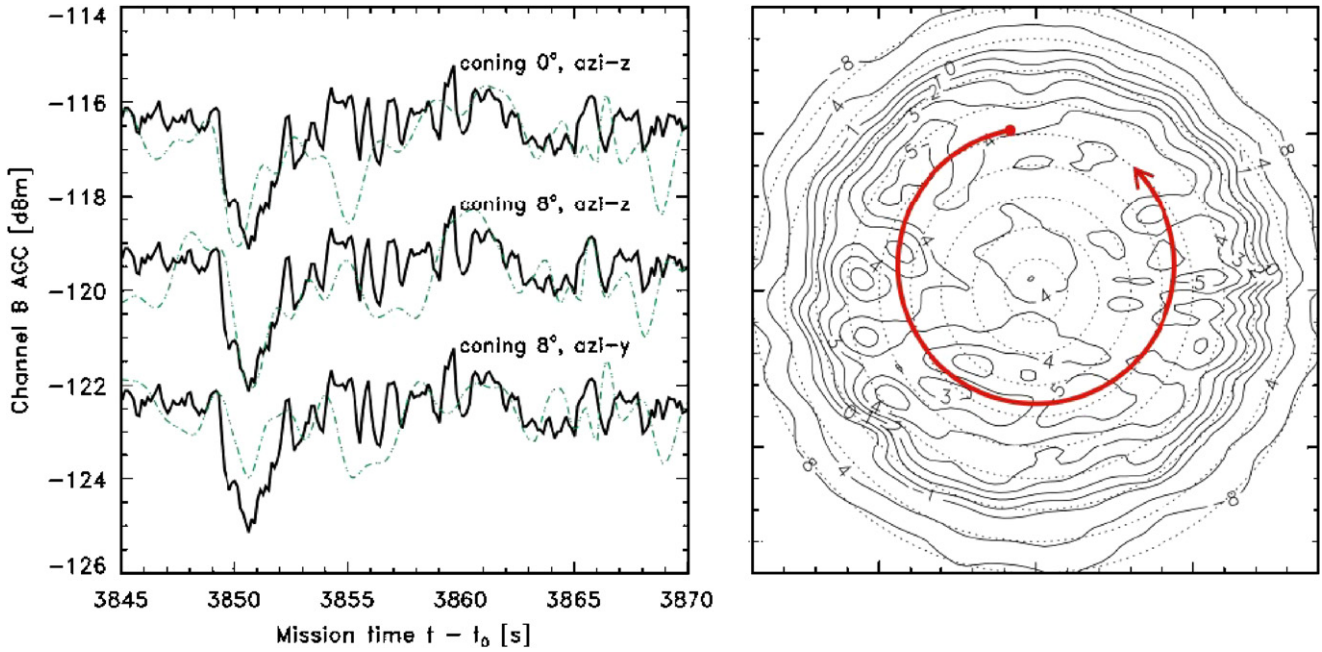


Fig. 10. Left panel: comparison of the measured Channel B AGC with the model results for different coning parameters shortly before 10:15 UTC (around 3850 s mission time). The measured AGC (solid curves) is compared to simulations with different coning angles and azimuths (dashed curves). The upper plot gives the simulation results for zero coning. The best fit (centre, lowered by 3 dB) is achieved for 8° coning, where the highest point on the experiment platform is on the z-axis ($\varphi_{\text{coning}} = 90^\circ$). To show the importance of choosing the correct coning azimuth in addition to the magnitude of the coning angle, a third simulation is shown (lowered for clarity by 6 dB), again for 8° coning angle, but the highest points on the y-axis ($\varphi_{\text{coning}} = 0^\circ$). The second model is clearly in best agreement with the data. Right panel: path described by the Cassini/Huygens line-of-sight vector in the antenna diagram during the time plotted, for the best-fit case. Note the 8° offset of the circular path from the antenna boresight in the direction of the +z-axis. The dot corresponds to mission time 3845 s; the arrowhead gives the position of the line-of-sight vector at mission time 3870 s and marks the direction of movement of the line-of-sight vector in the antenna diagram.

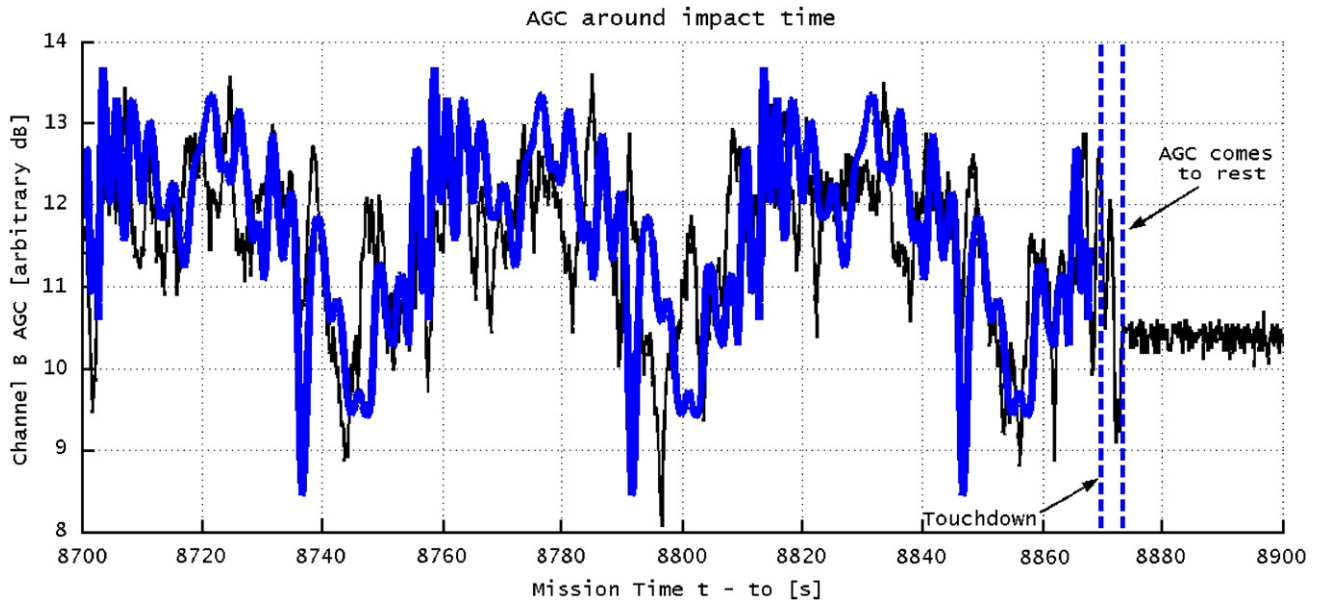


Fig. 11. Channel B AGC around the time of impact on Titan. The thin black solid curve is the observed AGC. The thick blue curve is the predicted AGC for a zero-tilt, zero-coning rotation in the antenna diagram at 70° PAA. After nominal impact at 8870 s mission time, the AGC continued to fluctuate until coming to rest at about 8873.5 s mission time.

last four periods before nominal impact of the probe. After nominal impact, the Channel B AGC variations are seen to continue for about 3.5 s before coming to rest. The

penetration probe of the Surface Science Package (SSP) dated the touchdown event at mission time 8870 s (Lebreton et al., 2005). Nevertheless, the Channel B

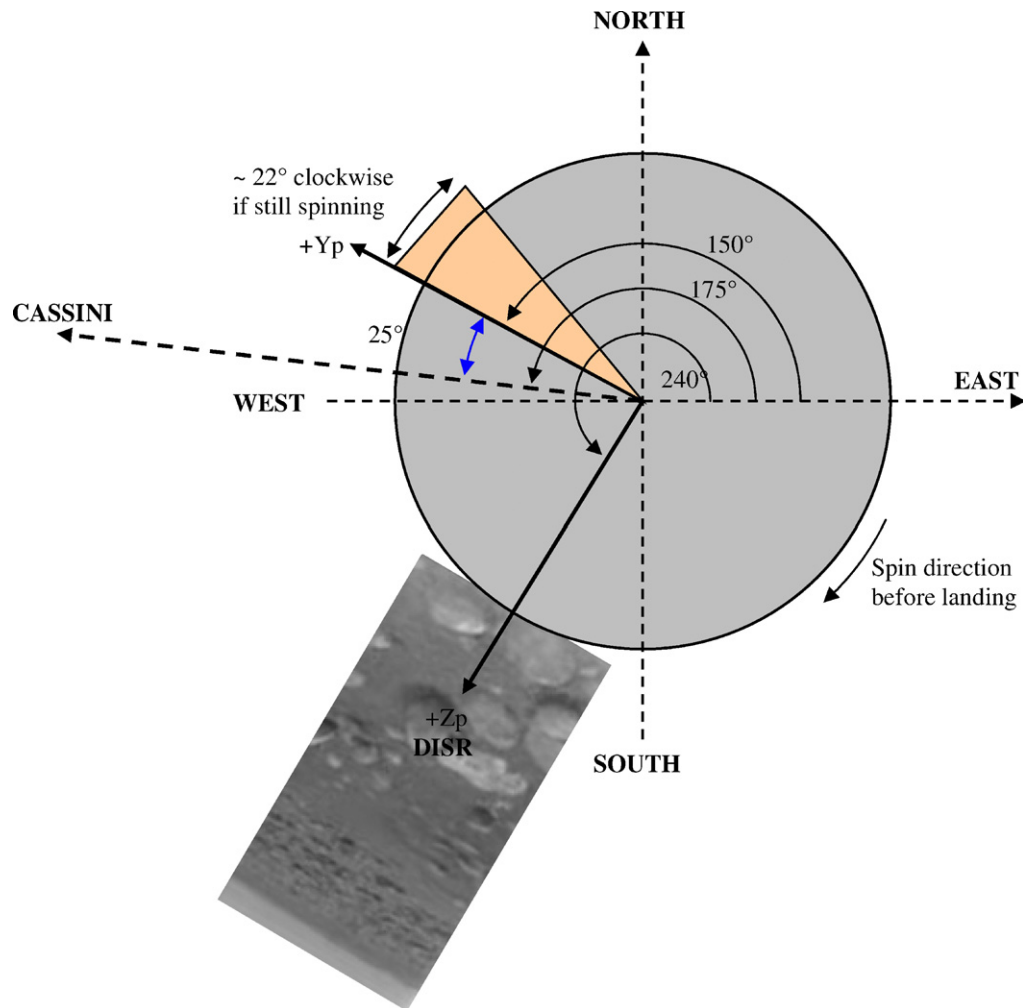


Fig. 12. Estimated landing orientation from the AGC data. At nominal impact, the azimuth of the Huygens y -axis was approximately 150° from east, i.e., 25° from the line-of-sight vector to Cassini. If the probe continued to spin for 3.5 s before coming to rest, it may have rotated by 22° if spinning with its pre-impact spin rate. In this case, the azimuth at impact would have been 128° . According to this analysis, the DISR imagers ($+z$ -axis) were thus directed at the azimuth 240° from east. The error associated with this analysis is $\pm 30^\circ$. This compares with the value $257 \pm 5^\circ$ from east derived by Karkoschka et al. (2007). The picture of the Titan surface was taken by DISR (NASA/ESA/University of Arizona).

frequency was observed to jump discontinuously at 8872 s (Pérez-Ayúcar et al., 2005). This event has been attributed to the shock of impact on the Channel B transmitter. Since the telemetry is time-stamped onboard Cassini and Huygens data are stamped on the Probe, the difference could be explained by a timing inaccuracy (under investigation). The touchdown event is marked in the accelerometer readings by a shock and a transitory oscillation until the measurements freeze. The transitory or bouncing phase lasts for several seconds.

Depending on whether or not the probe rotation is extrapolated linearly for this time, the azimuth of the y -axis at impact is determined to be between 150° and 125° (Fig. 12). The DISR study (Karkoschka et al., 2007) determined that the camera (i.e., the z -axis) was pointed to an azimuth corresponding to $257 \pm 5^\circ$ (SSW) in the system defined by Fig. 12 at impact. This agrees with the results from the Channel B AGC analysis to within its standard error, estimated to be $\pm 30^\circ$.

6. Conclusions

The Huygens Probe Channel B signal strength measured on Cassini was modelled for the Probe descent onto Titan using the known position and velocity of the Probe and Orbiter at every instant during the mission and accounting for Probe rotation, variable tilt and coning motion. It is shown that the main features of the Channel B AGC measurements can be explained by Probe rotation and east–west tilt excited by changes in zonal wind speed. Significant coning motion over long times can be excluded, even though individual rotation periods may indicate short-lived coning or tilt of the Probe, possibly due to buffeting of the Probe by winds. The model fit is sufficiently good to determine the direction of the Probe axes over most of the descent. Unfortunately, the quality of the simulation deteriorates near the surface prior to impact. Here, the data are in rough agreement with the DISR imager results, indicating

that the Probe z-axis was pointing approximately southwards.

Acknowledgements

This work presents results of a research project partially funded by the Deutsches Zentrum für Luft- und Raumfahrt (DLR). Y.D. thanks the Studienstiftung des deutschen Volkes for support during her thesis research.

References

- Allison, M., Ferri, F., Bird, M.K., Fulchignoni, M., Asmar, S.W., Atkinson, D.H., Colombatti, G., Tyler, G.L., 2005. A preliminary meteorological interpretation of correlated Huygens DWE and HASI data. *Bull. Amer. Astron. Soc.* 37 (3), 717.
- Bird, M.K., Allison, M., Asmar, S.W., Atkinson, D.H., Avruch, I.M., Dutta-Roy, R., Dzierma, Y., Edenhofer, P., Folkner, W.M., Gurvits, L.I., Johnston, D.V., Plettemeier, D., Pogrebenko, S.V., Preston, R.A., Tyler, G.L., 2005. The vertical profile of winds on Titan. *Nature* 438, 800–802.
- Dzierma, Y., 2005. Investigation of planetary winds by means of Doppler measurements: the Huygens Doppler Wind Experiment and its predecessors in the solar system. Diplomarbeit, University of Bonn.
- Folkner, W.M., Asmar, S.W., Border, J.S., Franklin, G.W., Finley, S.G., Gorelik, J., Johnston, D., Kerzhanovich, V.V., Lowe, S.T., Preston, R.A., Bird, M.K., Dutta-Roy, R., Allison, M., Atkinson, D.H., Edenhofer, P., Plettemeier, D., Tyler, G.L., 2006. Winds on Titan from ground-based tracking of the Huygens Probe. *J. Geophys. Res.* 111, E07S02, doi:10.1029/2005JE002649.
- Jones, J.C., Giovagnoli, F., 1997. The Huygens Probe system design. In: *Huygens: Science, Payload and Mission*, ESA SP-1177, pp. 25–45.
- Karkoschka, E., Tomasko, M., Doose, L., Rizk, B., See, C., McFarlane, L., Schröder, S., and the DISR team, 2007. DISR imaging and the geometry of the descent of Huygens. *Planet. Space Sci.*, this issue, doi:10.1016/j.pss.2007.04.019.
- Kazeminejad, B., Atkinson, D.H., Pérez-Ayúcar, M., Lebreton, J.-P., and the Huygens Descent Trajectory Working Group, 2007. Huygens' entry and descent through Titan's atmosphere: Methodology and results of the Huygens entry and descent trajectory reconstruction. *Planet. Space Sci.*, this issue, doi:10.1016/j.pss.2007.04.013.
- Lebreton, J.-P., Matson, D.L., 1997. The Huygens Probe: science, payload and mission overview. In: *Huygens: Science, Payload and Mission*, ESA SP-1177, pp. 5–24.
- Lebreton, J.-P., Witasse, O., Sollazzo, C., Blancquaert, T., Couzin, P., Shipper, A.-M., Jones, J.B., Matson, D.L., Gurvits, L.I., Atkinson, D.H., Kazeminejad, B., Pérez-Ayúcar, M., 2005. An overview of the descent and landing of the Huygens Probe on Titan. *Nature* 438, 758–764.
- Lorenz, R.D., Zarnecki, J.C., Towner, M.C., Leese, M.R., Ball, A.J., Hathi, B., Hagermann, A., Ghafoor, N.A.L., 2007. Descent motions of the Huygens Probe as measured by the Surface Science Package (SSP): turbulent evident for a cloud layer. *Planet. Space Sci.*, this issue, doi:10.1016/j.pss.2007.04.007.
- Pérez-Ayúcar, M., Sarlette, A., Couzin, P., Blancquaert, T., Witasse, O., Lebreton, J.-P., 2005. Huygens attitude reconstruction based on flight engineering parameters. Paper Presented at the Third International Planetary Probe Workshop, Anavyssos, Greece.
- Pérez-Ayúcar, M., Lorenz, R.D., Floury, N., Prieto-Cerdeira, R., Lebreton, J.-P., 2006. Bistatic observations of Titan's surface with the Huygens Probe radio signal. *J. Geophys. Res.* 111, E07001, doi:10.1029/2005JE002613.
- Sarlette, A., 2005. Characterization of the spin and attitude of the ESA Huygens Probe during its descent onto Titan using the engineering dataset. Graduation Thesis, Liège University.